Computer Science Department of The University of Auckland
CITR at Tamaki Campus (http://www.citr.auckland.ac.nz)

CITR-TR-81 August 2001

Determination of Geometric Parameters for Stereoscopic Panorama Cameras

Shou Kang Wei, Fay Huang, and Reinhard Klette[1]

Abstract

This paper proposes an approach for solving the parameter determination problem for a stereoscopic panorama camera. Image acquisition parameters have to be calculated under given constraints defined by application requirements, the image acquisition model, and specifications of the targeted 3D scenes. Previous studies on stereoscopic panorama imaging, such as [IYT92, MB95b, WHK99b, PPB00, SKS99, HWK01, Sei01, WP01], pay great attention on how a proposed imaging approach supports a chosen area of application. The image acquisition parameter determination problem has not yet been dealt with in these studies. The lack of guidance in selecting image acquisition parameters affects the validity of results obtained for subsequent processes [WHK00]. Our approach towards parameter determination allows to satisfying commonly demanded 3D scene visualization/reconstruction application requirements: proper scene composition in resultant images; adequate sampling at a particular scene distance; and desired stereo quality (i.e. depth levels) over a diversity of scenes of interest. The paper details the models, constraints and criteria used for solving the parameter determination problem. Some practical examples are given for demonstrating the use of the formulas derived. The study contributes to the design of stereoscopic panorama cameras as well as to manuals for on-site image acquisition. The results of our studies are also useful for camera calibration, or pose estimation in stereoscopic panoramic imaging.

[1] Center for Image Technology and Robotics Tamaki Campus, The University of Auckland, Auckland, New Zealand. shoukang, fay, r.klette@auckland.ac.nz

Determination of Geometric Parameters for Stereoscopic Panorama Cameras

Shou Kang Wei, Fay Huang and Reinhard Klette

CITR, Computer Science Department, The University of Auckland
Tamaki Campus, Auckland, New Zealand

Abstract

This paper proposes an approach for solving the parameter determination problem for a stereoscopic panorama camera. Image acquisition parameters have to be calculated under given constraints defined by application requirements, the image acquisition model, and specifications of the targeted 3D scenes. Previous studies on stereoscopic panorama imaging, such as [IYT92, MB95, WHK99, PPBE00, SKS99, HWK01b, Sei01, WP01], pay great attention on how a proposed imaging approach supports a chosen area of application. The image acquisition parameter determination problem has not yet been dealt with in these studies. The lack of guidance in selecting image acquisition parameters affects the validity of results obtained for subsequent processes [WHK00]. Our approach towards parameter determination allows to satisfying commonly demanded 3D scene visualization/reconstruction application requirements: proper scene composition in resultant images; adequate sampling at a particular scene distance; and desired stereo quality (i.e. depth levels) over a diversity of scenes of interest. The paper details the models, constraints and criteria used for solving the parameter determination problem. Some practical examples are given for demonstrating the use of the formulas derived. The study contributes to the design of stereoscopic panorama cameras as well as to manuals for on-site image acquisition. The results of our studies are also useful for camera calibration, or pose estimation in stereoscopic panoramic imaging.

Keywords: panorama camera, image acquisition, line camera, stereoscopic panorama.

1 Introduction

Image acquisition is a process for capturing light fields[1] in real 3D scenes, which is critical for subsequent image analysis and visualization processes [WHK00]. An *image acquisition model* defines image-acquiring components (e.g. different linear sensors rotating around a joint axis) and their

[1] All possible light rays in a specified 3D space and time interval form a *light field* [LH96, GGSC96]. A general function mapping light fields on measured intensities is called *plenoptical function* [AB91].

geometric relations during an image acquisition process. Image acquisition parameter determination characterizes basic geometric and/or photometric relations among application requirements, the image acquisition model, and specific constraints of the targeted 3D scenes.

Panorama cameras define a possible option for light field capturing [Che95, MB95, SS97, WHK99, PPBE00]. The panorama imaging approach is a logical solution for capturing light fields surrounding a single viewing point. Panoramic images (*panoramas* for short) are relevant to disciplines such as computer vision, computer graphics, or stereoscopic imaging and display.

Stereoscopic panoramas are designed to enhance 3D perception [WHK98, WHK99, PBE99, SKS99, Sei01]. Stereoscopic panoramas capture depth information in a special epipolar geometry defined by doubly-ruled surfaces[2]. Fundamental geometric studies for stereoscopic panoramas are reported in [SKS99, HWK00, HWK01b, Sei01, WP01]. Compared to studies for traditional imaging approaches, e.g. [HZ00], much more works still needs to be done for stereoscopic panoramas. This paper addresses the parameter determination problem of stereoscopic panorama imaging.

H. Ishiguro et al. first proposed an image acquisition model that is able to produce multiple panoramas by a single swiveling of a pinhole-projection camera, where each panorama is associated with multiple focal points. The model was proposed for the 3D reconstruction of an indoor environment. Their approach reported in 1992 in [IYT92] already details essential features of the multi-perspective panoramic image acquisition model. The modifications or extensions based on their model have been discussed by many others such as [HP00, PBE99, PPBE00, SH99, SKS99, SS99, WHK99]. A more comprehensive literature review for panoramic imaging approaches can be found in [WHK00].

Previous studies pay great attention on how the proposed imaging approach could support an area of application. The image acquisition parameter determination problem has not yet been dealt with. The analysis of relations between application requirements, image acquisition model and specification of the given 3D scenes is also not yet covered in the literature on panoramic imaging. Of course, it is valuable to control parameters of imaging system based on a given variety of 3D scenes. The lack of such studies affects the validity of results obtained for subsequent processes [WHK00].

The paper is organized as follows. Section 2 briefly reviews our basic stereoscopic panorama image acquisition model and the epipolar geometry of panoramas. Section 3 addresses application requirements for stereoscopic imaging, and specifies some criteria for image acquisition parameter determination methods. Section 4 introduces some supporting parameters/models to assist in constraining the image acquisition parameter determination process. Finally, Section 5 presents a precise approach to parameter determination. The paper ends with conclusions, especially for future work.

2 Acquisition Model

Our image acquisition model is also designed for covering the specification of near-scene/indoor panorama acquisition, defining special needs for controllability of depth levels (disparities) in resultant stereo pairs. Figure 1 shows one hardware realization of a panoramic camera, and [HWK01a, HKW+01] reports about technical data and experiments using recent line-camera technology.

[2]The only doubly-ruled surfaces in 3D space are the plane, the hyperboloid and the hyperbolic paraboloid [HCV91]. These surfaces allow that re-generated images are directly stereoscopic-viewable. They also support the reuse of stereo-matching algorithms, previously developed for binocular stereo images.

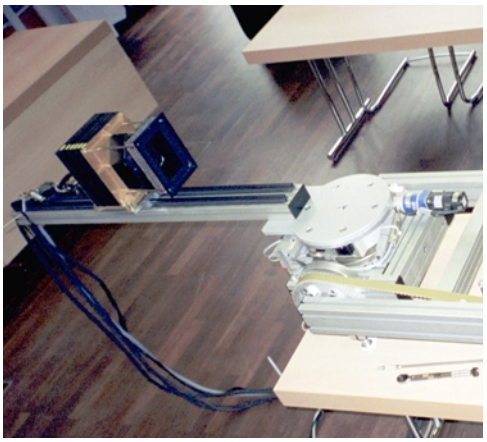

Figure 1: Stereoscopic panorama camera at the space sensory institute of DLR (German Aerospace Center).

Our model benefited from these practical experiences, and we were able to contribute to the design of these cameras. This paper reports about these contributions on a more theoretical level.

The conceptual model of stereoscopic panoramic image acquisition (using a line camera) is depicted in Fig. 2. Fundamental geometric studies for this model are reported in [HWK01a]. The focal point **C** of a slit camera [RS97] is rotated with respect to a rotation center **O**. The optical axis must pass through both **O** and **C**. The effective focal length, denoted as f, and the CCD element size (or pixel size), denoted as u, are assumed to be given.

The circle describing the path of all focal points during rotation is called *focal circle*. The distance between the slit camera's focal point and the rotation axis, denoted as R, remains constant for a stereoscopic panorama imaging process. The angular interval of every subsequent rotation step is assumed to be constant.

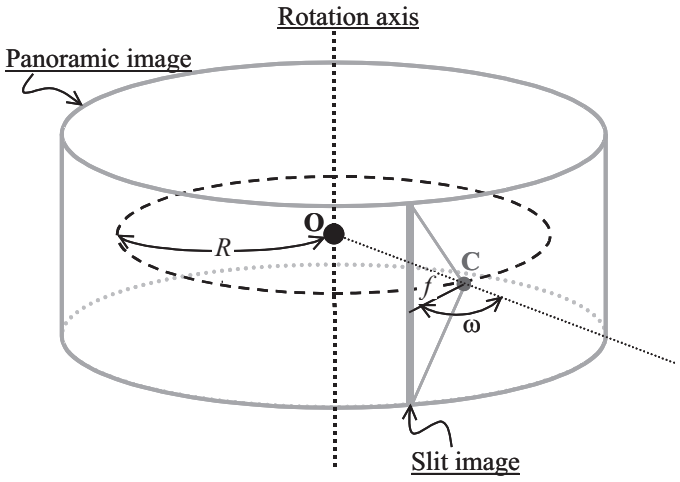

Figure 2: The stereoscopic panoramic imaging model. See text for details.

Each slit image contributes to one column of a panoramic image of dimension $W_P \times H_P$ in pixels. An angle, ω, is defined by the angle between the normal vector of the focal circle at the associated focal point, and the optical axis of the slit camera. The angle parameter provides a flexibility in capturing different viewing-angled panoramic images, which is known to be useful in various applications [PBE99, SH99].

A panoramic pair of ω and $(360^\circ - \omega)$ is referred to as *Symmetric Pair*. The epipolar geometry of such a pair is characterized by epipolar lines being image rows [HWK01a]. This paper focuses on the image acquisition parameter determination problem for this symmetric case.

In general, this model allows a uniform description of various previously proposed models for different applications, such as stereoscopic visualization [HH98, WHK99, PBE99], stereo reconstruction [IYT92, Mur95, KS97, HWK01b, SS99], or image-based rendering [Che95, MB95, KD97, RB98].

3 Requirements and Criteria

We consider two main demands for image acquisition: first, allow proper *scene composition* (coverage of 'important features', sufficient representation of geometric complexity etc.) in resultant images, and second, allow desirable depth levels (or spatial disparities) over a range of scenes of interest in the resultant images.

If a 3D scene of interest is not properly represented in resultant images, the acquired images may not be interpreted with good coherence between them. An imaging parameter determination method therefore needs to ensure that parameters are set such that the scene of interest appears in sufficient perspectives in the acquired images.

Insufficient resolution in disparities over the relevant interval of distance values, for a given 3D scene of interest, produces a cardboard effect [YOY00], i.e. the 3D scene is perceived as a set of parallel cardboards, sorted in depth, one sitting in front of the next one. On the other hand, depth levels greater than the upper disparity limit of human vision cause double images, called *dipopia*, which results in uncomfortable stereo viewing as well as eyestrain [Vii97, STA99, MNKL00]. An image acquisition parameter determination method therefore needs to ensure that parameters allow desirable depth levels (or spatial disparities) in resultant images, over a variety of 3D scenes of interest.

Image acquisition is a time-consuming, storage-consuming[3] and costly[4] task/process. Without having a proper image acquisition parameter determination method at hand, the quality of resultant images cannot be ensured. Further acquisitions might be required and will incur more costs.

Sometimes we may also encounter time/storage-critical situations (e.g. limited time/storage capacities) that do not allow us to take as many images as we want. Any image acquisition parameter determination method should be portable and time-efficient. In general, such a method should be simple (small number of steps involved), accessible and affordable.

[3] For instance, one panoramic image is of 3.4 giga-byte size in [HKW+01].

[4] Labor, equipment, transportation, insurances etc. are expensive.

4 Supporting Parameters and Constraints

To meet the requirements and criteria previously mentioned, we need to introduce some supporting parameters/models to be imposed as constraints to regularize the parameter-determination process of stereoscopic panorama imaging. This section discusses the assumptions, definitions, concepts, practical considerations, and the valid ranges of the supporting parameters/models.

4.1 Scene Range of Interest

Image acquisition at one location is a way of composing a specific range/region of a 3D scene of interest into resultant images. We need a model describing varieties of 3D scenes of interest.

We propose a simple model of concentric cylinders, which is illustrated in Fig. 3, as seen from the top. The area between the smaller and the larger dashed circles stands for the *region of interest* (*RoI* in short), i.e. accurate distance values or stereo visualizations are desirable for this region. The nearest and the furthest distances of the RoI are denoted as D_1 and D_2, and $D_1 < D_2$. Our RoIs do have a base area like an annulus, however, the height is very important as well, especially for allowing scene composition. We discuss our approach of modeling the height of RoI in the next section. Using the furthest and the nearest objects of interest to specify the range of interest

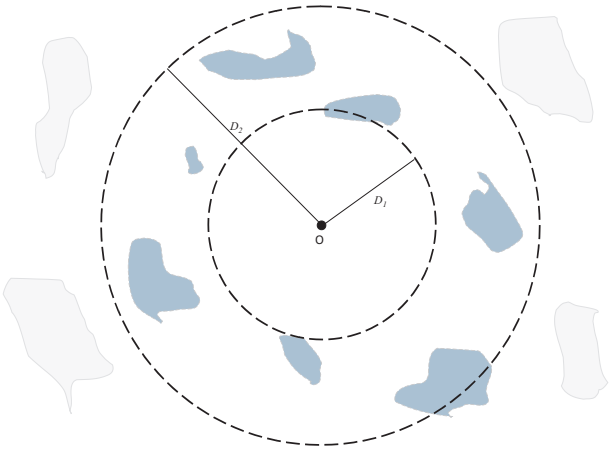

Figure 3: Top view of the concentric cylinder model for describing a RoI. Darker (blue) objects indicate locations which are primarily of interest while lighter (gray) areas are not or less of interest. The two dashed circles describe the RoI and are defined by their radiuses.

matches related intuitions. The range can be read from a distance-measuring device.

4.2 Distance of Camera to Target Range

To allow a proper scene representation in the resultant images, two important factors need to be considered first. The first is the positioning of the imaging-system in respect to the RoI. The second is the choice of lens angles to capture all desirable scene objects. For instance, the vertical *angular field of view* [5] (FOV in short) of the lens is wider/narrower and the distance between a

[5]For a panorama, the horizontal angular field of view has no impact on scene composition. But the vertical angular FOV is very important for allowing sufficient scene composition in resultant images.

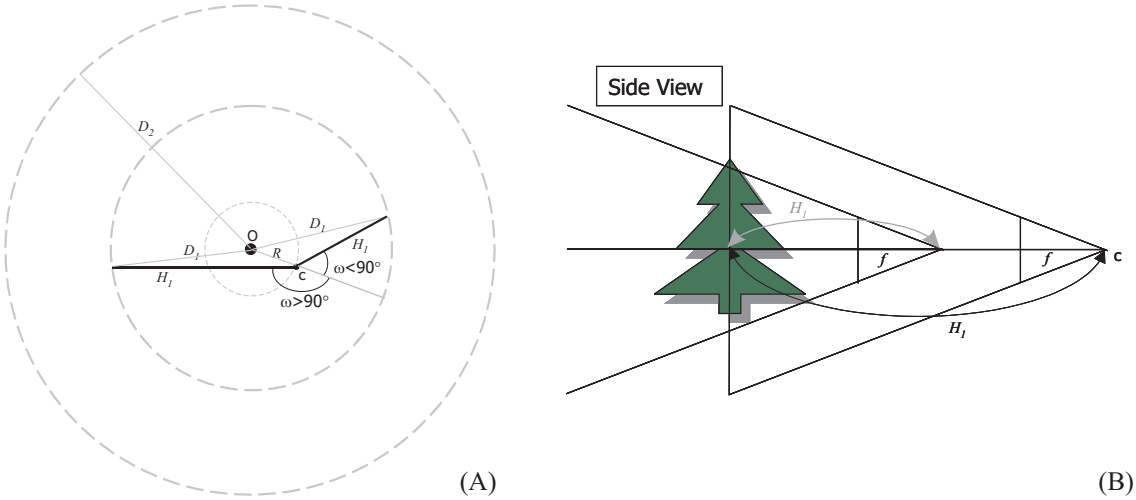

(A) (B)

Figure 4: (A) illustrates the definition of H_1 via two examples: closer to the target range (i.e. $\omega < 90°$ on the right) and further away from the target range (i.e. $\omega > 90°$ on the left). (B) shows how different H_1 values (in light and dark colors) can affect the scene composition in an image with respect to the intended target.

camera and the RoI in a 3D scene is longer/shorter, the bigger/smaller the height[6] of the RoI is.

Because both factors are subjective and content-dependent, we leave the choices to the system user and use the distance between camera and RoI for modeling. The main difficulties of positioning an imaging system in practice are spatial and temporal limitations, that is, we cannot set a system anywhere at anytime as we want. And regarding the lens angles, the availability of varieties are usually quite limited. This paper assumes that the positioning of the camera is pre-determined and a desired lens of a fixed-angle is chosen and available.

In order to compose the RoI of a scene properly between D_1 and D_2, in resultant images, the distance between $\mathbf{C}$ and any point on the cylinder of D_1 needs to be estimates and kept constant for a 360° panorama acquisition. We denote the distance by H_1. Figure 4 (A) illustrates the two examples H_1: closer and further to the target range. Figure 4 (B) shows how different H_1 can affect the scene composition with respect to the intended target (i.e. a tree in the figure).

A wide-angle lens is often chosen for a near scene. Lens distortion cannot be avoided in this case, which is unfortunate especially for visualization applications. In the stereoscopic panoramic image acquisition model, the parameters R and ω allow to have a flexible H_1 such that a longer H_1 permits a less wide-angle lens to be used and hence results in reduced lens distortion.

Practically H_1 is estimated in a similar way as for D_1 and D_2. The valid range of H_1 is the minimum focusable distance $< H_1 < 2 \times D_1$.

4.3 Resolution

Unlike the single-center panoramic imaging approach [Che95, MB95, KW97] where the number of image columns is determined independent from the 3D scene complexity, the number of image

[6]The height of RoI is defined at distance of D_1 in this paper.

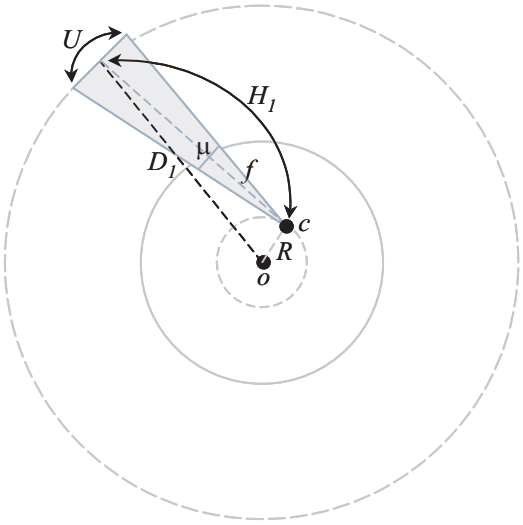

Figure 5: Geometric model of computing the horizontal spatial image resolution W_P of a stereoscopic panorama. See text for details.

columns of a stereoscopic panorama [IYT92, WHK98, WHK99, PBE99, SH99] may vary depending on the geometric relation between the imaging system and the 3D scene of interest. Note that this relation has not been studied or even mentioned in previous publications.

Figure 5 illustrates the geometric model for computing the horizontal resolution W_P of a stereoscopic panorama. Let a cylinder of D_1 be the uniform sampling target, and U be the —emphground sampling distance (GSD) demanded in the relevant application. The formula for computing W_P of a 360° panorama is as follows,

$$W_P = \frac{2\pi D_1}{U} \,. \tag{1}$$

Given an effective focal length f, a pixel size u, and the estimation of the corresponding value H_1, Eq. 1 can be rewritten as,

$$W_P = \frac{2\pi D_1}{U} = \frac{2\pi f D_1}{H_1 u} = \frac{2\pi f}{u}\frac{D_1}{H_1} \,. \tag{2}$$

The term $\frac{2\pi f}{u}$ in Eq. 2 gives the horizontal sampling rate for the single-center panorama case. It also shows that the calculation of the number of image columns in the single-center panorama case only involves camera parameters.

The term $\frac{D_1}{H_1}$ in Eq. 2 characterizes the main difference and the relation of the resolution calculation between single-center panorama and stereoscopic panorama. It also indicates which geometric relationships between the imaging system and the 3D scene of interest are required to be known.

For the special case that $\frac{D_1}{H_1} = 1$, where the stereoscopic panorama has the same number of image columns as the single-center panorama, stereoscopic panoramic imaging allows a more flexible sampling of orientations than single-center panoramic imaging. The circle $\mathcal{H}$ in Fig. 9

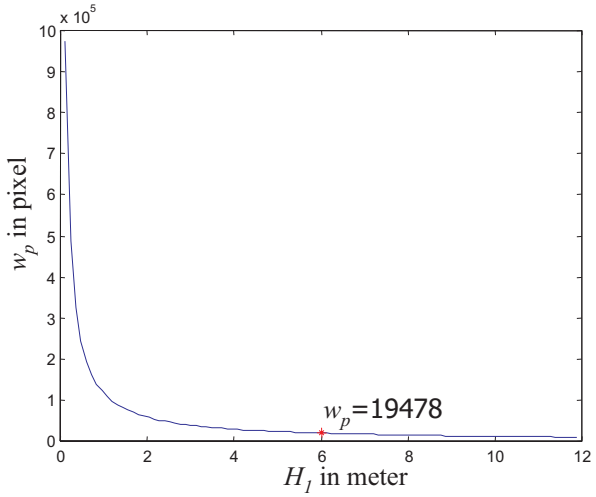

Figure 6: The results of horizontal resolution W_P determined for different H_1values (from 1.2m to 12m) and a sampling target at $D_1 = 6m$ for the camera of $f = 21.7mm$, $u = 0.007mm$, $H_P = 5184$ pixels. See text for further details.

illustrates the path of theoretically-possible sampling orientations along which scene points $\mathbf{P}_1$ can be sampled.

Since the resolution W_P limits the possible depth level/disparity in the resultant stereoscopic images, we assume $W_P > d_r$, where d_r is the disparity range (see the definition in Sec. 4.4) required by an application. This assumption is feasible and affordable in practice.

Figure 6 plots the results of stereoscopic panorama resolution determined for different H_1values (from 1.2m to 12m) at uniform sampling target of $D_1 = 6m$ for the camera WAAC [RS98] developed by DLR, where $f = 21.7mm$, $u = 0.007mm$, $H_P = 5184$ pixels. The resolution of $W_P = 19478$ pixels is used for a 12m $\times$ 12m seminar room at the space sensory institute of DLR, Berlin [HKW+01]. The resultant stereoscopic panoramic pair is shown as an anaglyph in Fig. 7.

Figure 7: Anaglyph of the stereoscopic panorama of the seminar room in DLR, Berlin.

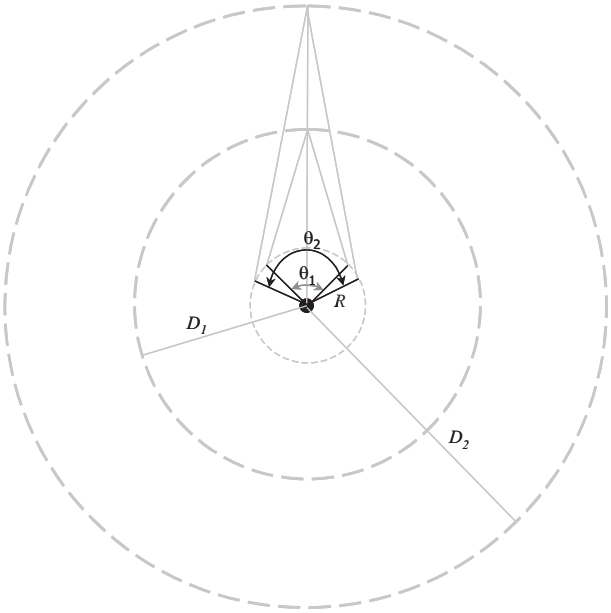

Figure 8: Example of two angular disparities θ_1 and θ_2 corresponding to two arbitrary 3D points of distances D_1 and D_2. See text for details.

4.4 Depth Level, Disparity, and Angular Disparity

Given a stereoscopic panoramic pair of resolution W_P, there is a finite number of depth levels within the range between D_1 and D_2. Two representations of depth levels are used in this paper. The first is called *angular disparity* which defines the angle of the two lines passing through **O** and the projections of a 3D corresponding point. Figure 8 depicts two angular disparities of two 3D points at distances D_1 and D_2 from **O**. The two angular disparities are denoted as θ_1 and θ_2. The angular disparity range is defined by $\theta_r = \theta_2 - \theta_1$.

The second representation is spatial disparity in image space, which has been well defined in conventional computer vision text books, see e.g. [KSK98]. We denote the disparities d_1 and d_2 as corresponding to θ_1 and θ_2. Similarly, $d_r = d_2 - d_1$ for the disparity range between the scene range D_1 and D_2 in image space. Note that d_r is one-dimensional for a symmetric pair. The conversion between θ_r and d_r is

$$\theta_r = \frac{2\pi d_r}{W_P}. \tag{3}$$

The valid ranges of θ_r and d_r are $0° < \theta_r < 180°$ and $0 < d_r < \frac{W_P}{2}$.

In designing a stereoscopic imaging system, it is necessary to include a function that allows that the desired depth levels may be set within the intended scene range (e.g. D_1 to D_2 in our case). In our stereoscopic panorama imaging model, the parameters R and ω provide such a function/access. Section 5 discusses how these two parameters are determined to meet the depth level requirement.

The number of depth levels, i.e. θ_r or d_r is basically application-specific. For stereoscopic visualization applications, the number of depth levels needs to satisfy both constraints of maximum human visual disparity [Val66] and of fusibility [HR95] under a particular viewing condition and a

viewing distance in respect to the size of a display screen [RS00, WGP98]. For instance, the number of depth levels in terms of pixels for a 17" screen (1024x768 pixels) viewing at 40cm frontal position is approximately $d_r \approx 70$ pixels for fusible and comfortable stereoscopic visualization [SN00].

For 3D reconstruction applications, the number of depth levels within the target range of a 3D scene must be at least above the lower bound (or the least acceptable) accuracy of the reconstruction. Note that the number of depth levels/disparities available in the region of interest of a stereoscopic pair limits the reconstruction accuracy regardless of the performance of the chosen stereo matching algorithms.

To produce proper depth levels in resulting perceived imagery is one of the key factors of quality stereoscopic perception. We notice that there is still a lack of understanding of human vision with respect to the enormous variety of binocular fusibility and viewing conditions, and limited characteristics of display methods etc. suggest that it is still difficult in calculating proper depth levels and accessing the quality. The calculation for obtaining $d_r \approx 70$ pixels uses the upper disparity limit suggested by [Val66], i.e. $0.03\times$ viewing distance, and assumes perceived imagery over both crossed and uncrossed disparity fields [HR95]. The examples given in the following sections assume the use of this particular value as depth level constraint for demonstration purposes.

5 Determination Formulation

Assume that D_1, D_2, H_1, and θ_r are given. What are possible choices of R and ω? This section answers this question by presenting a geometric analysis of the problem and the solution/formula for parameter derivation. The practical examples provided at the end of the section demonstrate the results of the parameter determination under given conditions in commonly appearing situations.

5.1 Geometrical Analysis

Figure 9 illustrates the symbols, definitions and geometric relations used in the following discussions. Let $\mathbf{P}_1$ and $\mathbf{P}_2$ be two points on the cylinders of radiuses D_1 and D_2 centered at $\mathbf{O}$. Let the points $\mathbf{P}_1$, $\mathbf{P}_2$ and $\mathbf{O}$ be collinear.

To ensure that the desired scene objects captured at $\mathbf{P}_1$ meet the composition requirement on the resulting image, the camera has to be constantly positioned at a distance H_1 away from the object. A circle centered at point $\mathbf{P}_1$ of radius H_1 defines the possible locations of the camera while acquiring the object at $\mathbf{P}_1$. Denote this circle as $\mathcal{H}$.

To allow the required number of depth levels within the intended range of a scene of interest on the resultant symmetric pair, the angular disparity range needs to be equal to θ_r. In other words, if a slit camera at $\mathbf{C}_1$ capturing a scene point $\mathbf{P}_1$, then after $(\theta_r/2)$ degrees of rotation with respect to the rotation axis shown in Fig. 2 the camera should be at $\mathbf{C}_2$ capturing a scene point $\mathbf{P}_2$ with a constant viewing angle ω, and vice versa.

To summarize, by combining the two above-mentioned geometric constraints, the parameter determination problem is to find R and ω such that $\mathbf{C}_1$ is on the circle $\mathcal{H}$ centered at point $\mathbf{P}_1$ and $\mathbf{C}_2$ has angular disparity range $(\theta_r/2)$ with respect to $\mathbf{C}_1$ while capturing the scene point $\mathbf{P}_2$.

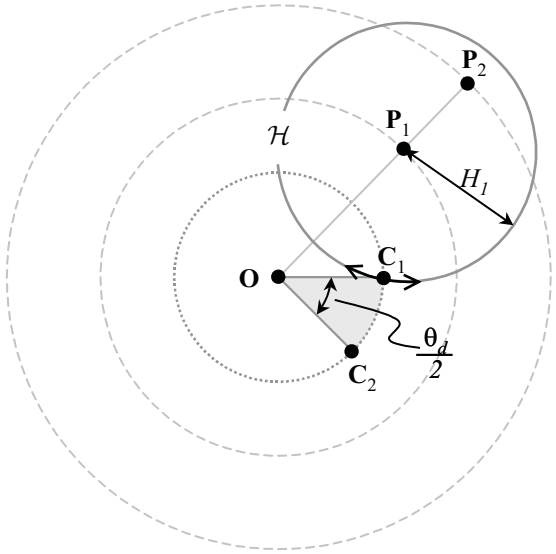

Figure 9: Geometric interpretation of finding possible R and ωvalues. See text for details.

5.2 Solution Derivation

Assume that the constraint parameters D_1, D_2, H_1, and θ_r, derived from a requirement analysis, are given. This section presents the formulas for finding related R and ω values. Figure 10 depicts the geometrical situation and the parameters used.

The possible range of a solution of R is $0 < R < D_1$. However, practically R should be less than or equal to the maximum length supported by the imaging system (e.g. 1m in [HKW+01]). For the solution of ω, only the range of $0° < \omega < 180°$ needs to be considered. Because ω is geometrically symmetric to the normal of the focal circle, so if ω is a solution, then $(360° - \omega)$ is also a solution. Note that $R = 0$ or $\omega = 0°$ or $180°$ do not support capturing a stereoscopic panorama.

The two triangles $\triangle \mathbf{OP}_1\mathbf{C}_1$ and $\triangle \mathbf{OP}_2\mathbf{C}_2$ in Fig. 10 can be transformed such that the point $\mathbf{C}_1$ coincides with the point $\mathbf{C}_2$ (i.e. a rotation transformation of θ_r degrees with respect to $\mathbf{O}$). The geometry of these two triangles after the transformation is depicted in Fig. 11. Let angle $\angle \mathbf{OP}_1\mathbf{P}_2$ be denoted as ϕ, and angle $\angle \mathbf{OP}_1\mathbf{C}_2$ be denoted as δ (i.e. $\delta = (180° - \phi)$).

In $\triangle \mathbf{OP}_1\mathbf{P}_2$, the length of the side $\overline{\mathbf{P}_1\mathbf{P}_2}$, dented as L, can be calculated by the following formula:

$$L = \sqrt{D_1^2 + D_2^2 - 2D_1D_2\cos\theta_r}.$$

Again, in $\triangle \mathbf{OP}_1\mathbf{P}_2$, the angle ϕ has the following relationship with the three sides of the triangle:

$$\begin{aligned} \cos\phi &= \frac{D_1^2 + L^2 - D_2^2}{2D_1L}, \\ &= \frac{D_1^2 + D_1^2 + D_2^2 - 2D_1D_2\cos\theta_r - D_2^2}{2D_1\sqrt{D_1^2 + D_2^2 - 2D_1D_2\cos\theta_r}}, \\ &= \frac{D_1 - D_2\cos\theta_r}{\sqrt{D_1^2 + D_2^2 - 2D_1D_2\cos\theta_r}}. \end{aligned} \tag{4}$$

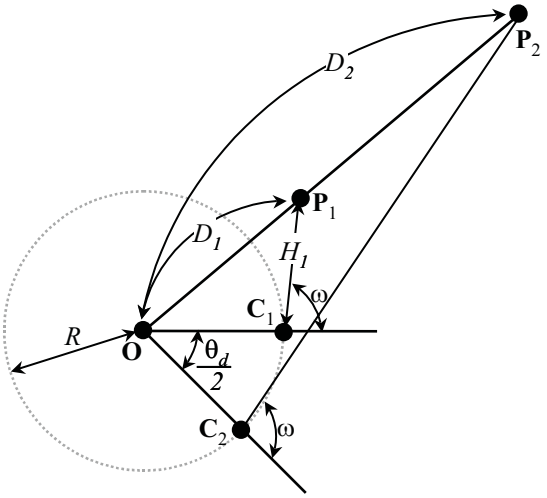

Figure 10: The basic geometry of our parameter-determination solution. See text for more details.

The angle δ is defined to be equal to $(180° - \phi)$, thus we have

$$\begin{aligned} \cos\delta &= \cos(180° - \phi), \\ &= -\cos\phi. \end{aligned} \tag{5}$$

In $\triangle \mathbf{OP}_1\mathbf{C}_2$, R can be calculated using the following formula:

$$R = \sqrt{D_1^2 + H_1^2 - 2D_1H_1\cos\delta}.$$

Summarizing the results from Eq. 4 and Eq. 5, the value of R can be obtained as follows:

$$R = \sqrt{D_1^2 + H_1^2 + 2D_1H_1\frac{D_1 - D_2\cos\theta_r}{\sqrt{D_1^2 + D_2^2 - 2D_1D_2\cos\theta_r}}}.$$

In $\triangle \mathbf{OP}_1\mathbf{C}_2$, the angle ω satisfies the following equation:

$$\begin{aligned} D_1^2 &= R^2 + H_1^2 - 2RH_1\cos(180° - \omega), \\ &= R^2 + H_1^2 + 2RH_1\cos\omega. \end{aligned}$$

Once the value of R is computed, the angle ω can be calculated as follows:

$$\omega = \arccos\left(\frac{D_1^2 - H_1^2 - R^2}{2H_1R}\right).$$

5.3 Examples

Four examples of commonly occurring situations are given to demonstrate the results of the determined parameters R and ω. The examples include (1) a small indoor scene covering an area of about $36m^2$; (2) a bigger indoor scene of an area of about $400m^2$; (3) an outdoor or open-area scene with a closer range of interest of about 6 to 50 meters from the center; (4) and an outdoor

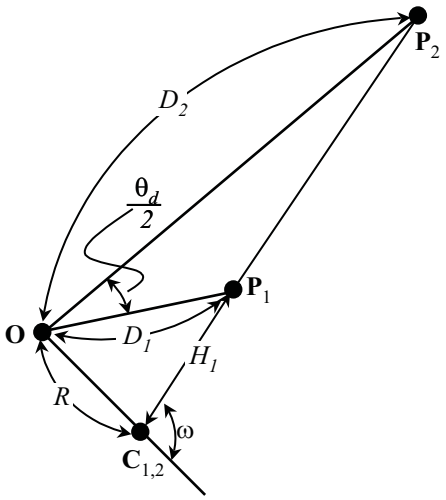

Figure 11: The transformed geometry of the parameter-determination solution derivation. See text for more details.

scene with a further range of interest of about 20 to 200 meters from the center. The determination results, shown in Tab. 1, of R and ω for the four different cases are calculated based on the specifications of the equipment (e.g. WAAC) and the setups described in [HKW+01].

The supporting parameters include the effective focal length $f = 21.7mm$, pixel size $u = 0.007mm$, panoramic image height $H_P = 5184$ in pixels, and the display screen height $H_S = 768$ in pixels. To allow that acquired stereoscopic panoramas are directly fusible and viewing is comfortable at a specific display screen resolution, Eq. 3 becomes

$$\theta_r = \frac{2\pi d_r H_P}{W_P H_S},$$

where $d_r = 70$ pixels are used in all four cases for a 17" display screen (1024x768 pixels) viewing at 40cm frontal position over both crossed and uncrossed disparity fields. The parameters D_1, D_2, H_1 and R are measured in meters, θ_r and ω in degrees, and W_P in pixel.

	D_1	D_2	H_1	W_P	θ_d	R	ω
(1)	1	3	1.2	16232	10.48	0.2499	146.88
(2)	4	10	4.2	18550	9.17	0.5809	113.92
(3)	6	50	5.5	21249	8.00	0.6768	44.66
(4a)	20	200	20.0	19478	8.74	1.6942	92.43
(4b)	20	200	20.0	19478	5.00	0.9695	91.39
H_P = 5184 (pixels) H_S = 768 (pixels)				u = 0.007 (mm) f = 21.7 (mm)			

Table 1: The results of the determined parameters R and ω and the given conditions in four typical examples: (1) small indoor scene; (2) bigger indoor scene; (3) near outdoor scene; (4a) and (4b) larger outdoor scene. See text for further explanations.

The results of the determined parameters R and ω in Tab. 1 show the actual values satisfying the scene-composition and depth-level requirements under the given conditions. The parameter ω in the first two examples illustrates the adaptation to indoor (close-scene) conditions, that is, $\omega > 90°$ (a slit-camera faces inwardly with respect to **O**). Such flexibility provides a great value to this imaging system applied in practice.

The parameter R computed in the example (1-3) is actually realizable using the setup in [HKW+01], i.e. the value of R can be set up to 1m. The example (4a) has an impractical case where R is over 1m. We demonstrate the tradeoff to the depth-level requirement by reducing θ_r from 8.74° to 5.00° for $R < 1m$.

6 Conclusions and Future Work

The solution of the parameter determination problem is unique. This implies neither R nor ω can match application requirements satisfactorily alone.

Although the parameters R and ω introduce a more complicated panorama acquisition system, they enable a control to adapt the system to different 3D scene conditions. In particular, the flexibilities such as allowing different sampling orientations, different composition flexibilities and the lens distortion reduction are exclusively advantageous to a near-scene stereoscopic panorama imaging in practice.

Our approach of the parameter determination allows meeting the commonly demanded 3D scene visualization/reconstruction application requirements: proper scene composition in resultant images; adequate sampling at a particular scene distance; and desired stereo quality (i.e. depth levels) over a range of scenes of interest.

The study allows proper parameters to be determined at acquisition time (accessibility) such that the subsequent processes could be simplified, e.g. it supports directly viewable stereo. The proposed determination method can be applied easily in both indoor and outdoor situations (portability). Our approach allows the acquisition to perform only once to get the desired results and require only three distance estimations, which can be done easily with a commercially available binocular (time-efficient and affordable).

Practically, the study can serve as reference for stereoscopic panoramic imaging camera design, or as base-knowledge for designing WYSIWYG user interfaces for interactive parameter determination and also an on-site acquisition guide. Theoretically, our study provides a new treatment in dealing with interactions between an imaging system and 3D scene complexity and the results may be useful for further studies such as calibration, or pose estimation of panoramic imaging.

Future work should answer the following analysis questions: what are the main factor(s) influencing the determination results and how to evaluate these influences (factor analysis)? Since R and ω have limited intervals in reality, which limits of scene range and depth levels are admissible (limit analysis)? How the estimation errors of D_1, D_2, and H_1 would affect/violate the satisfaction of the requirements (error analysis)?

Acknowledgments

The first author thanks the space sensory institute of DLR (German Aerospace Center) for an efficient research visit in March 2001 allowing a further specification of our panoramic camera

model in accordance with recent line camera technologies.

References

[AB91] E.H. Adelson and J.R. Bergen. The plenoptic function and the elements of early vision. In *Computational Models of Visual Proceeding*, pages 3–20, Cambridge, Massachusetts, USA, 1991.

[Che95] S. E. Chen. QuickTimeVR - an image-based approach to virtual environment navigation. In *Proc. SIGGRAPH'95*, pages 29–38, Los Angeles, California, USA, August 1995.

[GGSC96] S.J. Gortler, R. Grzeszczuk, R. Szeliski, and M.F. Cohen. The lumigraph. In *Proc. SIGGRAPH'96*, pages 43–54, New Orleans, Louisiana, USA, August 1996.

[HCV91] D. Hilbert and S. Cohn-Vossen. *Geometry and the Imageination.* AMS, Chelsea, Providence, RI, 1991.

[HH98] H.-C. Huang and Y.-P. Hung. Panoramic stereo imaging system with automatic disparity warping and seaming. *GMIP*, 60(3):196–208, 1998.

[HKW+01] F. Huang, R. Klette, S. K. Wei, A. Brner, R. Reulke, M. Scheele, and K. Scheibe. Hyper-resolution and polycentric panorama acquisition and experimental data collection. Technical Report Technical Report, CITR-TR-90, Centre for Image Technology and Robotics, The University of Auckland, New Zealand, May 2001.

[HP00] F. Huang and T. Pajdla:. Epipolar geometry in concentric panoramas. Technical Report Research Report CTU–CMP–2000–07, Center for Machine Perception, Czech Technical University, Prague, Czech Republic, March 2000.

[HR95] I.P. Howard and B.J. Rogers. *Binocular Vision and Stereopsis. Oxford Psychology Series No.29.* Oxford University Press, New York, 1995.

[HWK00] F. Huang, S.-K. Wei, and R. Klette. Epipolar geometry in polycentric panoramas. In *Multi-image analysis*, pages 40–51, Dagstuhl, Germany, March 2000.

[HWK01a] F. Huang, S. K. Wei, and R. Klette. Geometrical fundamentals of polycentric panoramas. In *Proc. ICCV01*, pages 560–565, Vancouver, Canada, July 2001.

[HWK01b] F. Huang, S.-K. Wei, and R. Klette. Stereo reconstruction from polycentric panoramas. In *Proc. Robot Vision 2001*, pages 209–218, Auckland, New Zealand, February 2001.

[HZ00] R. Hartley and A. Zisserman. *Multiple View Geometry in Computer Vision.* Cambridge Uni. Press, United Kingdom, 2000.

[IYT92] H. Ishiguro, M. Yamamoto, and S. Tsuji. Omni-directional stereo. *PAMI*, 14(2):257–262, 1992.

[KD97] S.-B. Kang and P.K. Desikan. Virtual navigation of complex scenes using clusters of cylindrical panoramic images. Technical Report Technical Report CRL 97/5, Digital Equipment Corporation, Cambridge Research Lab, WhereUnknown, September 1997.

[KS97] S.-B. Kang and R. Szeliski. 3-d scene data recovery using omnidirectional multibaseline stereo. *IJCV*, 25(2):167–183, 1997.

[KSK98] R. Klette, K. Schlüns, and A. Koschan. *Computer Vision - Three-Dimensional Data from Images*. Springer, Singapore, 1998.

[KW97] S.-B. Kang and R. Weiss. Characterization of errors in compositing panoramic images. In *Proc. CVPR97*, pages 103–109, San Jaun, Puerto Rico, USA, June 1997.

[LH96] M. Levoy and P. Hanrahan. Light field rendering. In *Proc. SIGGRAPH'96*, pages 31–42, New Orleans, Louisiana, USA, August 1996.

[MB95] L. McMillan and G. Bishop. Plenoptic modeling: an image-based rendering system. In *Proc. SIGGRAPH'95*, pages 39–46, Los Angeles, California, USA, August 1995.

[MNKL00] U. Mayer, M. D. Neumann, W. Kubbat, and K. Landau. Is eye damage caused by stereoscopic displays? In *Proc. SDVRS VII*, pages 4–11, San Jose, California, USA, January 2000.

[Mur95] D.W. Murray. Recovering range using virtual multicamera stereo. *CVIU*, 61(2):285–291, 1995.

[PBE99] S. Peleg and M. Ben-Ezra. Stereo panorama with a single camera. In *Proc. CVPR99*, pages 395–401, Fort Collins, Colorado, USA, June 1999.

[PPBE00] S. Peleg, Y. Pritch, and M. Ben-Ezra. Cameras for stereo panoramic imaging. In *Proc. CVPR00*, pages 208–214, Hilton Head Island, Jime 2000.

[RB98] P. Rademacher and G. Bishop. Multiple-center-of-projection images. In *Proc. SIGGRAPH'98*, pages 199–206, Los Angeles, California, USA, August 1998.

[RS97] R. Reulke and M. Scheel. Ccd-line digital imager for photogrammetry in architecture. *nt. Archives of Photogrammetry and Remote Sensing*, XXXII(5C18):195–201, 1997.

[RS98] R. Reulke and M. Scheel. Der drei-zeilen ccd-stereoscanner waac: Grundaufbau und anwendungenin der photogrammetrie. *Photogrammetrie, Fernerkundung, Geoinformation*, 3:157–163, 1998.

[RS00] J. W. Roberts and O. T. Slattery. Display characteristics and the impact on usability for stereo. In *SPIE Proc. Stereoscopic Displays and Virtual Reality Systems VII*, pages 128–137, San Jose, California, USA, January 2000.

[Sei01] S. M. Seitz. The space of all stereo images. In *Proc. ICCV01*, pages 26–33, Vancouver, Canada, July 2001.

[SH99] H.-Y. Shum and L.-W. He. Rendering with concentric mosaics. In *Proc. SIGGRAPH'99*, pages 299–306, Los Angeles, California, USA, August 1999.

[SKS99] H. Shum, A. Kalai, and S. Seitz. Omnivergent stereo. In *Proc. ICCV99*, pages 22–29, Korfu, Greece, September 1999.

[SN00] M. Siegel and S. Nagata. Just enough reality: comfortable 3-d viewing via microstereopsis. *IEEE Trans. on Circ. and Sys. for Video Tech.*, 10(3):387–396, 2000.

[SS97] R. Szeliski and H.-Y. Shum. Creating full view panoramic image mosaics and environment maps. In *Proc. SIGGRAPH'97*, pages 251–258, Los Angeles, California, USA, August 1997.

[SS99] H.-Y. Shum and R. Szeliski. Stereo reconstruction from multiperspective panoramas. In *Proc. ICCV99*, pages 14–21, Korfu, Greece, September 1999.

[STA99] M. Siegel, Y. Tobinaga, and T. Akiya. Kinder gentler stereo. In *SPIE Proc. Stereoscipic Displays and Applications X*, pages 18–27, San Jose, California, USA, January 1999.

[Val66] N. A. Valyrus. *Stereoscopy.* Focal Press, London, 1966.

[Vii97] E. Viire. Health and safety issues for vr. *Communications of the ACM*, 40(8):40–41, 1997.

[WGP98] C. Ware, C. Gobrecht, and M. Paton. Dynamic adjustment of stereo display parameters. *IEEE Tran. on Systems, Man and Cybernetics, Part A*, 28(1):56–65, 1998.

[WHK98] S.-K. Wei, F. Huang, and R. Klette. Color anaglyphs for panorama visualizations. Technical Report Technical Report, CITR-TR-19, Centre for Image Technology and Robotics, The University of Auckland, New Zealand, February 1998.

[WHK99] S.-K. Wei, F. Huang, and R. Klette. Three-dimensional scene navigation through anaglyphic panorama visualization. In *Proc. CAIP99*, pages 542–549, Ljubljana, Slovenia, September 1999.

[WHK00] S.-K. Wei, F. Huang, and R. Klette. Classification and characterization of image acquisition for 3d scene visualization and reconstruction applications. In *Multi-image analysis*, pages xx–yy, Dagstuhl, Germany, March 2000.

[WP01] T. Werner and T. Pajdla. Cheirality in epipolar geometry. In *Proc. ICCV01*, pages 548–553, Vancouver, Canada, July 2001.

[YOY00] H. Yamanoue, M. Okui, and I. Yuyama. A study on the relationship between shooting conditions and cardboard effect of stereoscopic images. *IEEE Tran. on Circuits and Systems for Video Technology*, 10(3):411–416, 2000.